Variational Monte Carlo evaluations of Gutzwiller states for the Anderson-lattice model

P. G. McQueen
Department of Physics and Center for Superconducting Research, University of Maryland, College Park, Maryland 20742 and Complex Systems Theory Branch, Naval Research Laboratory, Washington D.C. 20375-5000

C. S. Wang
Department of Physics and Center for Superconducting Research, University of Maryland, College Park, Maryland 20742
(Received 26 November 1990; revised manuscript received 13 May 1991)

The electronic ground states for two- and three-dimensional Anderson-lattice clusters with large Hubbard repulsion are determined variationally within the Gutzwiller ansatz by use of a stochastic algorithm for exact evaluation of matrix elements of Gutzwiller states. The algorithm is similar to one normally used for finite-temperature simulation and is described in some detail. Variational states for a variety of Hamiltonian parameters and particle densities were considered. Of particular interest is the regime of small interband hopping, which is antiferromagnetic at densities near two particles per unit cell. We found that for some Hamiltonian-parameter regimes, doping the antiferromagnetic cluster with enough particles or holes can destroy the magnetic ordering and produce a state that resembles a heavy-Fermi-liquid state, a metal with a strongly-frequency-dependent self-energy. For a 4×4 Anderson lattice, we present results of low-temperature quantum Monte Carlo simulations to evaluate the validity of the variational Gutzwiller ansatz.

I. INTRODUCTION

The Anderson lattice is an extension of the Anderson model[1] which describes the formation of local moments in systems of dilute transition-metal impurities in nonmagnetic hosts. In the lattice model, the electrons that occupy the localized (f) orbitals interact among themselves through hybridization with an extended (d) band. We use a version of the Hamiltonian in which the d band has a tight-binding dispersion, with one f level for each d level:

$$H=\sum_{\mathbf{k}}\sum_{s}\varepsilon(\mathbf{k})d^{\dagger}_{\mathbf{k}s}d_{\mathbf{k}s}+V\sum_{\mathbf{r}}\sum_{s}(d^{\dagger}_{\mathbf{r}s}f_{\mathbf{r}s}+f^{\dagger}_{\mathbf{r}s}d_{\mathbf{r}s})$$
$$+E_f\sum_{\mathbf{r}}\sum_{s}n_{f\mathbf{r}s}+U\sum_{\mathbf{r}}n_{f\mathbf{r}\uparrow}n_{f\mathbf{r}\downarrow}\ , \qquad (1)$$

where the d band is taken as a simple tight-binding band:

$$\varepsilon(\mathbf{k})=2t[\cos(k_x)+\cos(k_y)+\cdots]\ .$$

The $\mathbf{k}$'s are the points of the first Brillouin zone, the $\mathbf{r}$'s label the real-space lattice sites, and s is the spin quantum number. E_f is the on-site energy of the localized f band; the hybridization between the two bands is described by a single hopping parameter V. A Hubbard interaction with strength U acts on electrons on the f sites.

Although neither spin-orbit coupling nor a finite dispersion for the f band are present in this model, it is still a reasonable simplification of the true electronic band structure of the heavy-fermion materials, such as UPt_3 or $CeCu_6$. The localized f orbitals are due to the heavy U or Ce ions, and the repulsive Hubbard term models the Coulomb energy produced when a localized orbital is doubly occupied. For any model to describe "heavy-fermion" behavior correctly, the self-energy must have a strong frequency dependence in order to explain why the specific heat is so large in such materials, even though transport properties (which would be measures of the effective mass in a noninteracting band model) are not unusually large at all.[2] It has been an open question whether or not the Hubbard interaction by itself is enough to stabilize such a Fermi liquid as the normal ground state. (Two good review articles about the application of the Anderson model to the heavy-fermion materials are listed in Ref. 3.)

In the limit of $U=\infty$ and large spin degeneracy, diagrammatic and mean-field treatments of the slave-boson auxiliary-field model have been very fruitful.[4–7] But because the slave-boson methods are exact only in the large-spin-degeneracy limit and because the random-phase approximation for finite but large U is believed to have some failings,[8] the case of small spin degeneracy is not as well understood. Various fermionic simulation schemes have been applied to the Anderson-lattice model.[9–12] Unfortunately, Zhang[13] has reported, and our experience has confirmed, that if the simulation methods devised for the two-dimensional Hubbard model are applied to the Anderson lattice with small V, then spin-spin correlations do not equilibrate at low temperatures. This is the very parameter regime that is expected to model heavy-fermion behavior.

For ground-state properties there is an alternative approach: the variational principle. A simple variational ansatz for strongly correlated systems (those with a strong U) was suggested by Gutzwiller,[14] and in Sec. II the precise choice of a trial Gutzwiller state will be discussed. In Sec. III we shall review an stochastic algorithm for the exact evaluation of the properties of such correlated electron trial states, which are usually impossible to obtain analytically. In Secs. IV and V we present numerical results for a variety of Hamiltonian parameters and particle densities to indicate that there are indeed regimes for which two- and three-dimensional heavy Fermi liquids are energetically stable. In Sec. VI the results of a finite-temperature simulation on very small clusters are

compared to the properties of Gutzwiller states for those small systems. A brief summary of our calculations and their limitations is given in Sec. VII.

II. GUTZWILLER ANSATZ FOR THE ANDERSON LATTICE

The variational state we take as

$$|G\rangle = P_g|\Psi\rangle \ , \tag{2}$$

where

$$P_g = \prod_{\mathbf{r}} [1-(1-g)n_{f\mathbf{r}\uparrow}n_{f\mathbf{r}\downarrow}] \ .$$

P_g projects out some fraction of doubly occupied f sites, with the parameter g determined variationally. The state $|\Psi\rangle$ is an independent particle state which can contain additional variational parameters. (The historical development of the Gutzwiller approach has been reviewed by Vollhardt.[15]) We formulate this independent particle state as

$$|\Psi\rangle = \exp(hM + h_s M_s)|\psi_0\rangle \ , \tag{3a}$$

where

$$M = \sum_{\mathbf{r}} (n_{f\mathbf{r}\uparrow} - n_{f\mathbf{r}\downarrow})$$

and

$$M_s = \sum_{\mathbf{r}} \exp[i(r_x\pi + r_y\pi + \cdots)](n_{f\mathbf{r}\uparrow} - n_{f\mathbf{r}\downarrow}) \ .$$

M is the magnetic moment, and M_s is the staggered moment. Fictitious magnetic fields h and h_s serve as variational parameters to enforce magnetic ordering. The state $|\psi_0\rangle$ is the nonmagnetic ground state of the following two-band Hamiltonian:

$$\begin{aligned} H' = & \sum_{\mathbf{k}} \sum_{s} [\varepsilon(\mathbf{k}) - \mu_G] d^{\dagger}_{\mathbf{k}s} d_{\mathbf{k}s} \\ & + \eta V \sum_{\mathbf{r}} \sum_{s} (d^{\dagger}_{\mathbf{r}s} f_{\mathbf{r}s} + f^{\dagger}_{\mathbf{r}s} d_{\mathbf{r}s}) \\ & + (E_f - \mu_b - \mu_G) \sum_{\mathbf{r}} \sum_{s} n_{f\mathbf{r}s} \ . \end{aligned} \tag{3b}$$

H' is just the Hamiltonian in Eq. (2) with $U=0$, except that the interband hopping has been rescaled by variational parameter η and the f on-site energy has been shifted by variational parameter μ_b. The pseudochemical potential μ_G sets the particle density and is not a variational parameter. Altogether, there are five variational parameters: g, η, μ_b, h, and h_s.

The hybridized bands of H' will both have finite dispersion; in energy, one band is completely above the rescaled f-site energy $E_f - \mu_b$ and the other band completely below the rescaled f-site energy. For both bands the density of states is greatest for energies nearest the rescaled f-site energy. If

$$2Dt + E_f - \mu_b \gg 4\eta^2 V^2 \ ,$$

where D is the dimension of the lattice, then the energy gap between the bands of H' is

$$E_{\text{gap}} \approx \frac{2Dt\eta^2 V^2}{4D^2t^2 - (E_f - \mu_b)^2} \ . \tag{4}$$

Note that this gap is proportional to $(\eta V)^2$. If there are exactly two particles per unit cell, then the lower band of H' is occupied and the upper one empty. (Of course, this will not be true in $|G\rangle$ because of the effects of P_g.) Since the f-site energy E_f is closer to the top of the lower band, the smaller ηV, the more the f band tends to be occupied in this special density limit.

If $\eta = 0$ and $g = 0$ with exactly one electron on each f site and all other electrons in the d band, then the f sites have decoupled from the system. On thermodynamic grounds such "decoupled f-moment" states must be excluded as ground states because they are highly degenerate: The spins on the f sites can be in any configuration. At zero temperature the entropy would then be gigantic. If such states are the Gutzwiller states of lowest energy, then the Gutzwiller ansatz cannot describe the true ground state of the system.

III. MONTE CARLO EVALUATION OF GUTZWILLER STATES

The main difficulty in evaluating matrix elements of $|G\rangle$ is that P_g is not easily expressible in momentum space, while the real-space wave function of $|\Psi_0\rangle$ is a Slater determinant. The resulting wave function for $|G\rangle$ is in Jastrow form, and it is possible to calculate its matrix elements by weighing the determinant terms stochastically. This has been done for the Hubbard model[16–18] and for one-dimensional Anderson chains with infinite U.[19] In certain special cases for the one-band Hubbard model, such as one-dimensional chains and infinite-dimensional systems, analytic expressions for Gutzwiller matrix elements can be deduced by mapping the matrix elements into a field theoretical model.[20–22]

An alternate approach that we introduced earlier to analyze states for one-band Hubbard models[23] will be used here for the Anderson lattice with some minor modifications. The expectation value of operator A with $|G\rangle$ can be written as

$$\begin{aligned} A &= \langle G|A|G\rangle / \langle G|G\rangle = \langle \Psi|P_g A P_g|\Psi\rangle / \langle \Psi|P_g^2|\Psi\rangle \\ &= \lim_{\beta_G \to \infty} \frac{\text{tr}[\exp(hM + h_s M_s)\exp(-\beta_G H')\exp(hM + h_s M_s)P_g A P_g]}{\text{tr}[\exp(hM + h_s M_s)\exp(-\beta_G H')\exp(hM + h_s M_s)P_g^2]} \ . \end{aligned} \tag{5}$$

The trace is over the quantum-mechanical states of the system. $1/\beta_G$ is not related to any real temperature of the system; it is introduced so that the ground state of H' dominates the trace. (This expression is closely related to the field-theoretical mapping of Refs. 20–22: the norm $\langle G|G\rangle$ plays the role of a partition function.) The operator P_g^2 can be re-

placed with a field of Ising variables interacting with the f electrons by applying the following Hubbard-Stratanovitch transformation:

$$[1-(1-g)n_{f\mathbf{r}\uparrow}n_{f\mathbf{r}\downarrow}]^2=1-(1-g^2)n_{f\mathbf{r}\uparrow}n_{f\mathbf{r}\downarrow}$$
$$=\exp(-2\kappa n_{f\mathbf{r}\uparrow}n_{f\mathbf{r}\downarrow})$$
$$=\tfrac{1}{2}\sum_{\sigma_{\mathbf{r}}}\exp[\alpha\sigma_{\mathbf{r}}(n_{f\mathbf{r}\uparrow}-n_{f\mathbf{r}\downarrow})-\kappa(n_{f\mathbf{r}\uparrow}+n_{f\mathbf{r}\downarrow})]\ , \tag{6}$$

where $\kappa=-\ln(g)$ and $\cosh(\alpha)=\exp(\kappa)$. The Ising variable $\sigma_{\mathbf{r}}$ in each unit cell $\mathbf{r}$ takes the values $+1$ and -1. The algorithm of Blankenbecler, Scalapino, and Sugar for a finite-temperature simulation, the BSS algorithm,[24] can now be applied to weigh the contributions of each Ising configuration to $\langle G|G\rangle$, with one major difference. In finite-temperature simulations it is necessary to introduce a Trotter approximation of the operator $\exp(-\beta H)$ into a product of more easily handled exponential operators that effectively separates the Hubbard and kinetic-energy terms from one another, which introduces an imaginary Matsubara time index on the Ising variables. Thus there are many Ising variables per unit cell for a simulation calculation. No Trotter breakup is needed to apply the BSS algorithm to the variational calculation, and so there is only one Ising variable per unit cell.

To evaluate $\langle A\rangle$ if $[A,P_g]=0$, the formula developed by Hirsch for the Hubbard model[25] to weigh the contribution of each Ising configuration can be used without change, with $\langle G|G\rangle$ in place of the partition function. However, the results need to be rescaled if $[A,P_g]\neq 0$. For example, to calculate an expression such as $\langle d^{\dagger}_{\mathbf{r}\downarrow}f_{\mathbf{r}\downarrow}\rangle$, one must use the identity

$$[1-(1-g)n_{f\mathbf{r}\uparrow}n_{f\mathbf{r}\downarrow}]f_{\mathbf{r}\downarrow}[1-(1-g)n_{f\mathbf{r}\uparrow}n_{f\mathbf{r}\downarrow}]$$
$$=\tfrac{1}{2}[g\cosh^2(\alpha/2)]^{-1/2}$$
$$\times\sum_{\sigma_{\mathbf{r}}}\exp[h(\sigma_{\mathbf{r}})/2]f_{\mathbf{r}\downarrow}\exp[h(\sigma_{\mathbf{r}})/2]\ , \tag{7}$$

where

$$h(\sigma_{\mathbf{r}})=\alpha\sigma_{\mathbf{r}}(n_{f\mathbf{r}\uparrow}-n_{f\mathbf{r}\downarrow})-\kappa(n_{f\mathbf{r}\uparrow}+n_{f\mathbf{r}\downarrow})\ .$$

Similar identities hold for $f_{\mathbf{r}\uparrow}$, $f^{\dagger}_{\mathbf{r}\uparrow}$, and $f^{\dagger}_{\mathbf{r}\downarrow}$.

To apply the BSS algorithm to Gutzwiller states, $\beta_G t$ must be set to a large enough value so that no excited states of H' contribute to the matrix elements; typically, $\beta_G t=3\times 10^8$ was more than enough for the lattices we examined. A cutoff c_G is imposed on the eigenvalues of the operator $\exp(-\beta_G H')$ in order to control numerical instabilities that can propagate in the matrix-manipulation operations of the BSS algorithm.[26,27] The presence of negative eigenvalues of the number-density matrix is a good test of such instabilities. However, c_G must be large enough to keep the total number of particles fixed on an integer value. We found that c_G in the range ± 16–± 17 was large enough to fix the particle number of the cluster to within one part in 10^{-5} without the density matrix having negative eigenvalues.

For a given set of parameters $\{g,\eta,\mu_b,h,h_s\}$, we found that $\langle H\rangle$ will converge within a few hundred Monte Carlo sweeps through the Ising spin lattice, although two-particle static correlations might take a few thousand sweeps to converge to their final values. Thus it takes about an hour of Cray CPU time to search through the parameter space for the minimum energy on a lattice of $\simeq 10^2$ unit cells, and once the minimum is found, a longer Monte Carlo computation of several thousand sweeps is done to calculate the two-particle static correlations.

IV. SOME TWO- AND THREE-DIMENSIONAL GUTZWILLER STATES

We now discuss a numerical "experiment" with the Gutzwiller ansatz. For two- and three-dimensional unit-cell clusters, we determined the variational ground state for a particle density of $n=2$ per unit cell and then dope the cluster with either electrons or holes. The number of unit cells for the clusters was $N_c=64$, a numerically convenient one for this procedure. (In the next two sections we explicitly address finite-size effects.) We examined the following set of Hamiltonian parameters for this experiment:

(a) 8×8 for $V=2t$, $E_f=0$, $U=32t$;

(b) 8×8 for $V=t$, $E_f=-2t$, $U=32t$;

(c) 8×8 for $V=3t/8$, $E_f=-t/2$, $U=32t$;

(d) $4\times 4\times 4$ for $V=3t/8$, $E_f=-t/2$, $U=4t$.

At particle density $n=2$, it can be shown analytically that the ground state for $U=0$ is a semiconductor with short-ranged, nearest-neighbor antiferromagnetic correlations and that the nearest-neighbor correlation is weakened as the particle density is shifted away from $n=2$. Shiba has suggested that whatever magnetic correlations are present in the $U=0$ ground state will be amplified in the Gutzwiller state, but the symmetry of these correlations will not change.[19] Our own data seem to suggest this: Figure 1 is a plot of the variationally determined staggered "magnetic field" h_s versus particle density n, and we note that the variational ground state for case (a) at $n=2$ is magnetically unordered and quite similar to the $U=0$ semiconductor, but is an antiferromagnetic in the other three cases. For cases (b)–(d), doping the clusters away from $n=2$ does reduce h_s. We tried to dope these clusters with both enough electrons and enough holes to drive h_s to zero, thus destroying the magnetic ordering. It is interesting to note that changing n by a large enough amount would change the symmetry of the spin-spin correlations in the $U=0$ bands so that the strongest

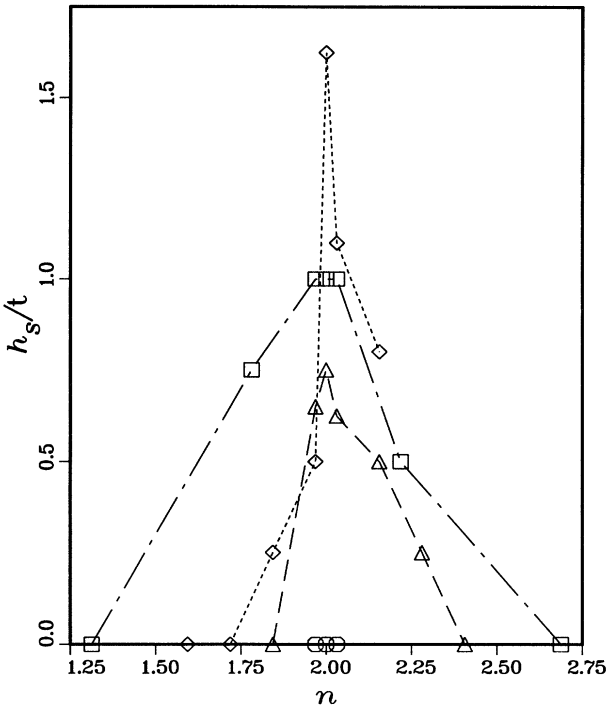

FIG. 1. Fictitious staggered magnetic field h_s vs the particle density per unit cell n. h_s/t is dimensionless. ○, cluster (a); △, cluster (b); ◇, cluster (c); and □, cluster (d).

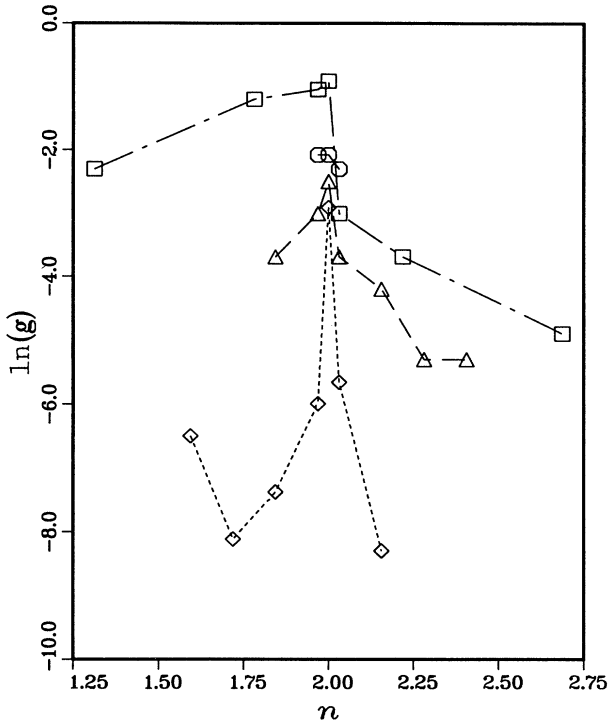

FIG. 2. Log of the Gutzwiller parameter g vs the particle density per unit cell n. Parameter g is dimensionless. ○, cluster (a); △, cluster (b); ◇, cluster (c); and □, cluster (d).

correlations would no longer be between nearest neighbors.

The smaller V's for cases (b)–(d) mean that the f-site occupation tends to be near unity for $n \approx 2$. In this regime one might expect the magnetic ordering of the f-site moments to allow electrons to hop between f sites (via hybridization with the d band), which lowers kinetic energy at the expense of the Hubbard energy. This is supported by Fig. 2, $\ln(g)$ as a function of n. The Gutzwiller projection parameter g has its maximum value (and the projection operator its weakest effects) for all cases at $n = 2$, where h_s is strongest. The actual f-site number occupation n_f of the variational states as a function of n is shown in Fig. 3. For cases (b) and (d), n_f rapidly decreases as n is reduced from 2, but in case (c), which has the smallest V of all, $n_f \approx 1$ for a greater range of n.

In cases (b)–(d), doping with electrons raises the d-electron occupation n_d above 1, while n_f is fixed near 1 to minimize the Hubbard interaction. The effective interband hopping ηV is shown in Fig. 4, a plot of $\ln(\eta V/t)$ vs n. Apparently, ηV is more sensitive to doping with electrons than with holes because doping with electrons increases double occupancy in the d band, which suppresses ηV due to the Pauli exclusion principle. The reduction in ηV reduces the effective f-f hopping. Thus the parameter g, which measures the probability of doubly occupied f sites, is suppressed by electron doping. The parameter g is also suppressed in case (c) when the cluster is doped with *holes*. Here $n_f \approx 1$, even as holes are added, and so n_d must drop quickly with particle density,

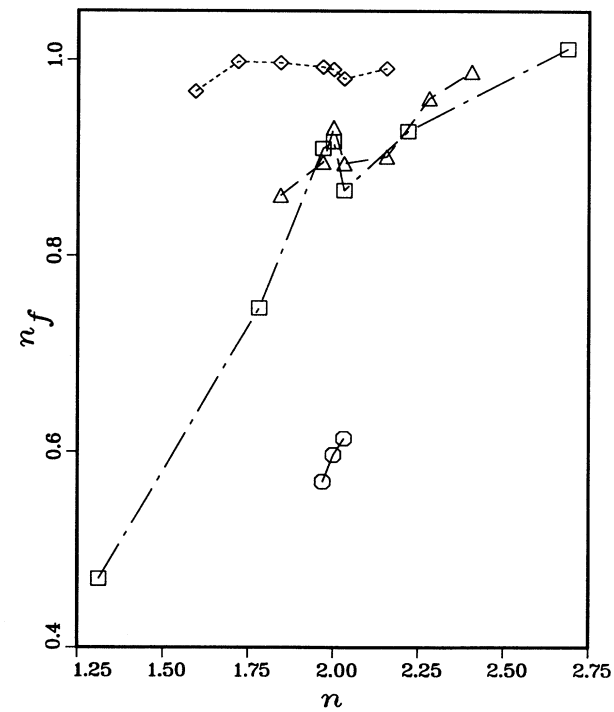

FIG. 3. f-site occupation per unit cell n_f vs the particle density per unit cell n. ○, cluster (a); △, cluster (b); ◇, cluster (c); and □, cluster (d).

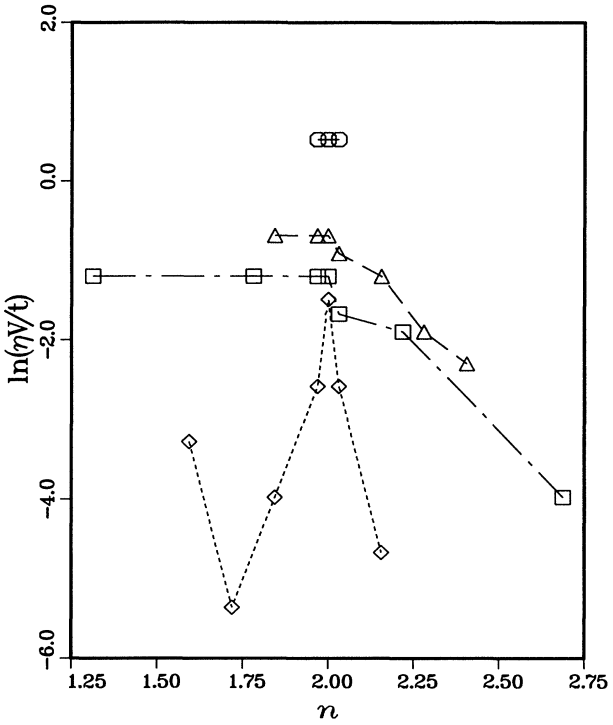

FIG. 4. Log of the effective interband hopping ηV vs the particle density per unit cell n. $\eta V/t$ is dimensionless. ○, cluster (a); △, cluster (b); ◇, cluster (c); and □, cluster (d).

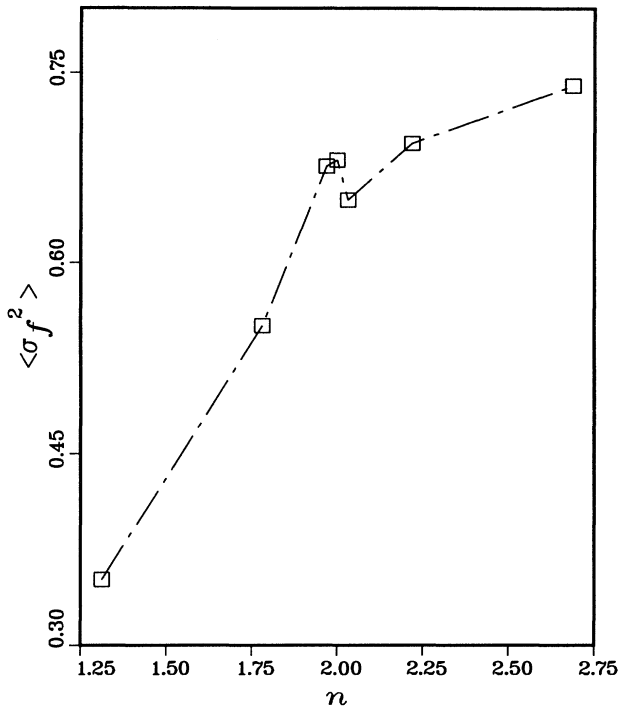

FIG. 5. f-site local moment $\langle \sigma_f^2 \rangle$ vs particle density per unit cell n for cluster (d). The local moment is dimensionless.

and the effective f-f hopping is reduced as fewer d electrons are available to mediate the f-f hopping. Again, the Gutzwiller projection must become stronger to doubly occupied f sites.

Closely related to the f-site density n_f is the f-site local moment $\langle \sigma_f^2 \rangle$, defined as

$$\langle \sigma_f^2 \rangle = \frac{3}{4N_c} \sum_{\mathbf{r}} \langle (n_{f\mathbf{r}\uparrow} - n_{f\mathbf{r}\downarrow})^2 \rangle$$

$$= \frac{3}{4} \left[n_f - \frac{2}{N_c} \sum_{\mathbf{r}} \langle n_{f\mathbf{r}\uparrow} n_{f\mathbf{r}\downarrow} \rangle \right] . \tag{8}$$

This quantity is also a measure of the density of doubly occupied f sites, and in a decoupled f-local-moment state would be exactly $\frac{3}{4}$. In clusters (a)–(c), $\langle n_{f\mathbf{r}\uparrow} n_{f\mathbf{r}\downarrow} \rangle \approx 10^{-3}$–$10^{-5}$, so that $\langle \sigma_f^2 \rangle$ is $\approx 75\%$ of n_f. U for cluster (d) is somewhat smaller, so that $\langle n_{f\mathbf{r}\uparrow} n_{f\mathbf{r}\downarrow} \rangle \approx 10^{-2}$. Figure 5 is a plot of $\langle \sigma_f^2 \rangle$ vs n for case (d), an example of this quantity mirroring n_f in these systems with strong Hubbard interactions.

The doping cluster (c) with particles drove the system into a density regime where the effective interband hopping ηV became so small that we could not tell within the numerical precision of our calculation whether or not the decoupled f-moment states are the favored states. Both the variationally determined estimate for the ground-state energy and the energy of the decoupled f-moment states are plotted as a function of n for case (c) in Fig. 6. Since the values of g and η for the other cases seem to be

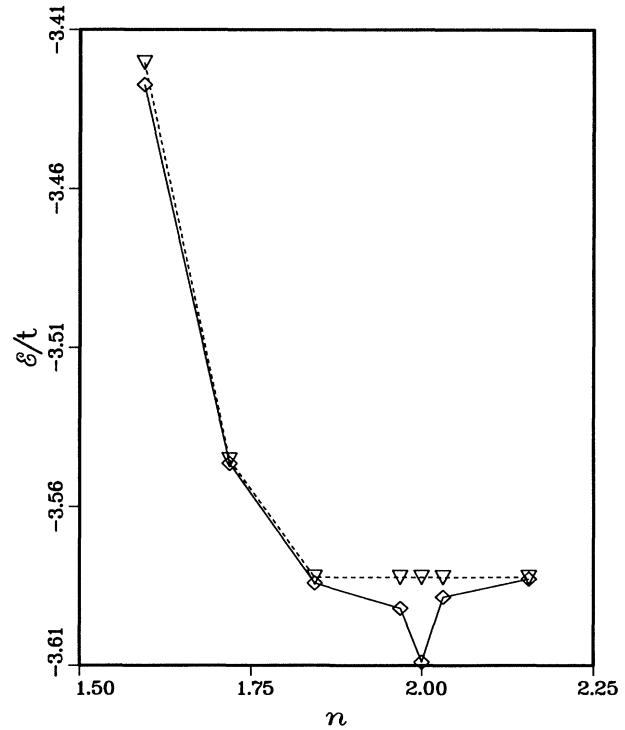

FIG. 6. Energy density E for cluster (c) vs particle density per unit cell n. E/t is dimensionless. ◇, E determined by the Gutzwiller variational ansatz; ▽, E for the decoupled f-local-moment states for cluster (b).

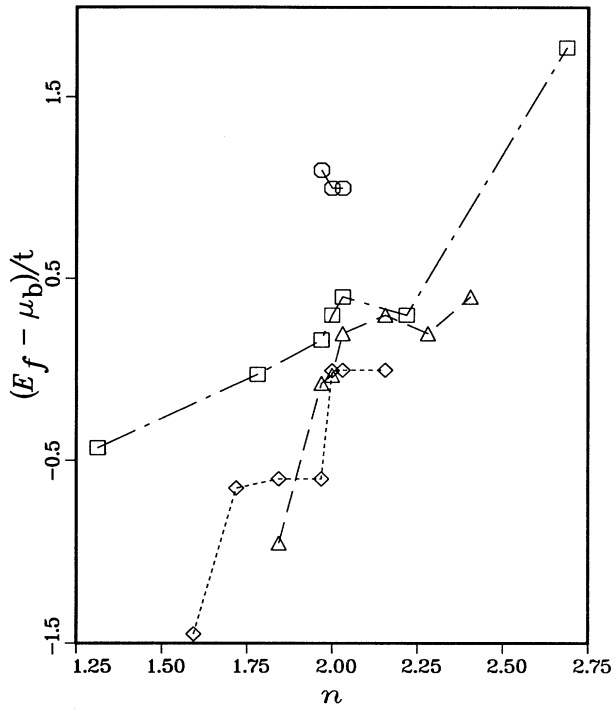

FIG. 7. Effective f on-site energy $E_f-\mu_b$ vs particle density per unit cell n. $(E_f-\mu_b)/t$ is dimensionless. ○, cluster (a); △, cluster (b); ◇, cluster (c); and □, cluster (d).

roughly exponential in n, it is unclear whether or not the decoupled f-moment states are really favored in cluster (c).

The effective f-site energy $(E_f-\mu_b)/t$ vs n of the clusters is plotted in Fig. 7, showing the behavior of this variational parameter. Also, we never found a density regime where a ferromagnetic state was favored.

V. HEAVY-FERMI-LIQUID STATE

By Luttinger's theorem[28] the Fermi surface of $|G\rangle$ is the same as that of $|\Psi\rangle$. Of course, finite clusters can have no true Fermi surface, but nontheless we know the discrete Fermi momenta in $|\psi_0\rangle$ for the clusters discussed above. There is another complication, though. Since this is a two-band system, the self-energy for spin s, $\Sigma_s(\mathbf{q},\omega)$, is really a 2×2 matrix:

$$\Sigma_s(\mathbf{q},\omega)=\begin{bmatrix}\Sigma_{sff}(\mathbf{q},\omega) & \Sigma_{sfd}(\mathbf{q},\omega)\\ \Sigma_{sdf}(\mathbf{q},\omega) & \Sigma_{sdd}(\mathbf{q},\omega)\end{bmatrix}. \tag{9}$$

The Hubbard interaction explicitly involves only the f electrons, and so $\Sigma_{sff}(\mathbf{q},\omega)$ will be the only nonzero component. However, the quasiparticle energies are the poles of the full 2×2 matrix Green's function, and so one must be careful in extracting quasiparticle properties from Σ_{sff}. Fortunately, Yip has found that there is still a relatively simple relationship between $\partial\Sigma_{sff}(\mathbf{q},\omega)/\partial\omega$ and the discontinuities in the components of the particle-density matrix at any momentum $\mathbf{q}$ on the Fermi surface.[29] Letting Δn_d and Δn_f be the jumps in the number occupation at Fermi vector $\mathbf{q}$ for the d and f bands (and one spin), respectively, then

$$1-\partial\Sigma_s(\mathbf{q},\omega)/\partial\omega|_{\omega=0}=(1-\Delta n_d)/\Delta n_f\ . \tag{10}$$

Although this relationship does not determine the mass enhancement, we would expect enhancement of the quasiparticle mass if $|\partial\Sigma_{sff}(\mathbf{q},\omega)/\partial\omega|$ is large.

TABLE I. Some properties of the metallic clusters created in the numerical doping experiment.

Cluster	n	$(1-\Delta n_d)/\Delta n_f$	$\langle\sigma_f^2\rangle$
(a)	1.968 75	1.42	0.423
(a)	2.031 25	1.55	0.457
(b)	1.843 75	3.45	0.645
(b)	2.406 25	31.3	0.745
(c)	1.593 75	14.3	0.726
(c)	1.843 75	244.0	0.749
(d)	1.3125	1.38	0.351
(d)	2.6875	24.6	0.740

Table I shows $(1-\Delta n_d)/\Delta n_f$ averaged over the Fermi momenta for the metallic systems discussed in Sec. IV above (or what would be metallic systems in the infinite-size limit). Also listed in Table I are the f-site local moments $\langle\sigma_f^2\rangle$ for each of these systems. In case (b) with $n=2.406\,25$, case (c) for $n=1.718\,75$ and $1.593\,75$, and case (d) with $n=2.6875$, Eq. (10) predicts that $|\partial\Sigma_{sff}(\mathbf{q},\omega)/\partial\omega|$ is at least an order of magnitude larger than in the other systems. These systems resemble metals with a self-energy that is strongly frequency dependent (a heavy Fermi liquid). The local f-site moments $\langle\sigma_f^2\rangle$ in these "heavy" metals are near $\frac{3}{4}$, its maximum value; also, the effective interband hopping ηV is very small. Although the local f-site moments are strong, the spin-spin correlations in the heavy-fermion-like clusters is *not* peaked for *nearest* neighbors, but for *next-nearest* neighbors. In all the "nonheavy" systems listed in Table I, the spin-spin correlations are peaked for nearest neighbors, except for cluster (d) with $n=1.3125$, but in this metal $\langle\sigma_f^2\rangle$ is very small. Apparently, the heavy Fermi liquid is the ground state of the Gutzwiller ansatz in systems with large U and small interband hopping whenever $n_f\approx1$, the f-site moment is strong ($\langle\sigma_f^2\rangle\approx\frac{3}{4}$), and the Fermi-surface structure of the underlying bands in $|\psi_0\rangle$ defeats nearest-neighbor antiferromagnetic ordering. This kind of state is called a "fluctuating moment" state, and we discuss it further in Sec. VII below.

Variational calculations performed for clusters with other Hamiltonian parameters and lattice sizes support this assertion about the formation of a heavy Fermi liquid. In finite-size clusters, it is not straightforward to compare the behavior of cluster of different sizes for density $n\neq2$ because the actual shape of the "Fermi surface" is a sensitive function of n, and clusters of different sizes do not support the same set of densities n. But it is still possible to examine clusters with size $N_c>64$, and the results for several addition clusters are summarized in Table II. For example, we considered 8×8 and 10×10 lattices with $V=3t/8$, $E_f=-t/2$, and $n\approx2.4$, so that

TABLE II. Properties of additional "metallic" clusters. $U=4t$ for all clusters.

Size	8×8	10×10	8×8	8×8
V/t	$\frac{3}{8}$	$\frac{3}{8}$	$\frac{3}{8}$	1
E_f/t	$-\frac{1}{2}$	$-\frac{1}{2}$	-2	-2
n	2.406 25	2.420 00	2.656 25	2.656 25
g	0.005	0.000 75	0.0035	0.27
μ_b/t	$-\frac{1}{5}$	-1.5	-2.35	-1.700
$\eta V/t$	$\frac{3}{160}$	$\frac{3}{800}$	$\frac{3}{400}$	$\frac{3}{5}$
n_f	0.998 74	0.998 74	1.000 54	1.26576
$\langle\sigma_f^2\rangle$	0.747	0.749	0.748	0.509
$(1-\Delta n_d)/\Delta n_f$	56.0	259.0	80.0	1.36

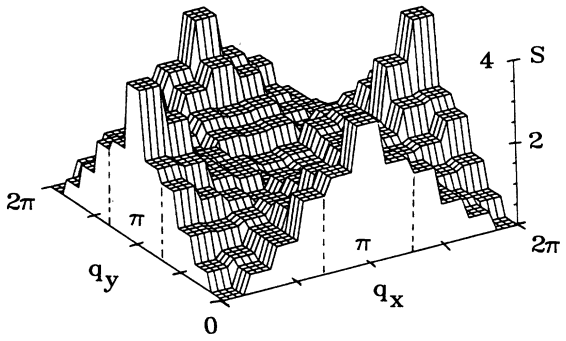

FIG. 9. Magnetic form factor $S(\mathbf{q})$ for a 10×10 cluster with $E_f=-t/2$, $V=t/2$, $U=4t$, and $n=2.42$.

$n_f\approx 1$. Then the Gutzwiller states for both size clusters have heavy-fermion characteristics. (However, the Fermi surface changes shape as the size is increased from 8×8 to 10×10, and so the values of the variational parameters are very different for the two sizes.) Figure 8 is a histogram of the particle-density matrix for the f band of the 10×10 cluster as a function of $\mathbf{q}$, and Fig. 9 is a similar histogram of the magnetic form factor $S(\mathbf{q})$. Note the tiny "jump" in the particle number at the edges of the cross in the center of the Brillouin zone in Fig. 8, which marks the location of the Fermi momenta, consistent with Luttinger's theorem. The form factor plotted in Fig. 9 corresponds to a real-space spin-spin correlation that is peaked for next-nearest neighbors. (Here, $S(\mathbf{q})$ is defined as

$$S(\mathbf{q})=\frac{1}{N_c}\sum_{\mathbf{r}_1}\sum_{\mathbf{r}_2}\exp[\mathbf{q}\cdot(\mathbf{r}_1-\mathbf{r}_2)]S(\mathbf{r}_1,\mathbf{r}_2)\ . \tag{11}$$

$S(\mathbf{r}_1,\mathbf{r}_2)$ is the spin-spin correlation between sites $\mathbf{r}_1$ and $\mathbf{r}_2$ for both the bands combined.)

We also considered an 8×8 cluster with $U=4t$ and $n=2.656\,25$. If $V=3t/8$ and $E_f=-t/2$, then the state resembles a heavy Fermi liquid. However, if E_f is lowered to $-2t$ and V raised to t, the state resembles an ordinary metal. In fact, for the latter set of parameters, $\langle\sigma_f^2\rangle=0.51$, which means that E_f is at such a low level compared to the Hubbard strength U that the Hubbard energy produced by the doubly occupied f sites is not large enough to affect the system very much. Again, the results are summarized in Table II.

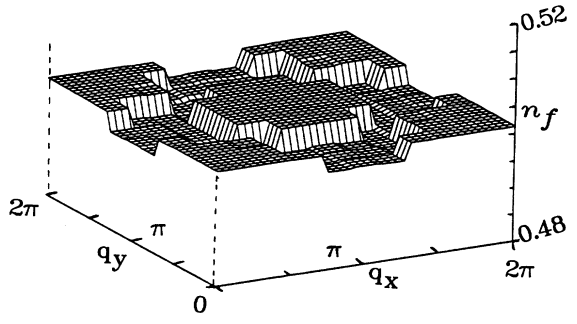

FIG. 8. f-band density matrix in momentum space for a 10×10 cluster with $E_f=-t/2$, $V=t/2$, $U=4t$, and $n=2.42$.

VI. TESTING THE VALDITY OF THE GUTZWILLER ANSATZ

As mentioned in Sec. I, finite-temperature simulations are of limited value when $V\ll t$, because spin-spin correlations will not equilibrate for temperature $T<t$, even after thousands of Monte Carlo sweeps through the lattice. Nonetheless, in order to test the validity of the Gutzwiller wave function, we attempted finite-temperature simulations with the BSS algorithm for very small (4×4) clusters with small V, using the BSS algorithm modified with Hirsch's technique to control numerical-error propagation.[26] Spin-spin correlations did not equilibrate, but $\langle H\rangle$ and the particle-density matrix certainly did equilibrate after a few thousands Monte Carlo sweeps. Thus we at least can compare the energy of Gutzwiller states for such small clusters to simulation results extrapolated to zero temperature.

Figure 10 shows the energy density per unit cell $E=\langle H\rangle/N_c$ as a function of temperature T for a 4×4 cluster with $n=2$, $U=4t$, $V=3t/8$, and $E_f=-2t$. This is a special choice of Hamiltonian parameters and density for which there will be exactly $\frac{1}{2}$ electrons per band per spin per unit cell for all T. Note that E converges nicely to the Gutzwiller value as $T\to 0$. Even better, the thermal ensemble averages of the components of H converge to their Gutzwiller expectation value as $T\to 0$. For example, the interband component k_{fd} to E, where

$$k_{fd}=\frac{1}{V}V\sum_{\mathbf{r}}\sum_{s}\langle f_{\mathbf{r}s}^{\dagger}d_{\mathbf{r}s}+d_{\mathbf{r}s}^{\dagger}f_{\mathbf{r}s}\rangle\ , \tag{12}$$

is shown in Fig. 11 as a function of T. The same thing is true for the f-site local moment $\langle\sigma_f^2\rangle$, plotted in Fig. 12 as a function of T. Note that $\langle\sigma_f^2\rangle$ has its maximum value at $T>0$, a Kondo-like behavior.

It seems that the $|G\rangle$ describes the ground state well for this cluster with $n=2$. However, $h_s\neq 0$, and so the

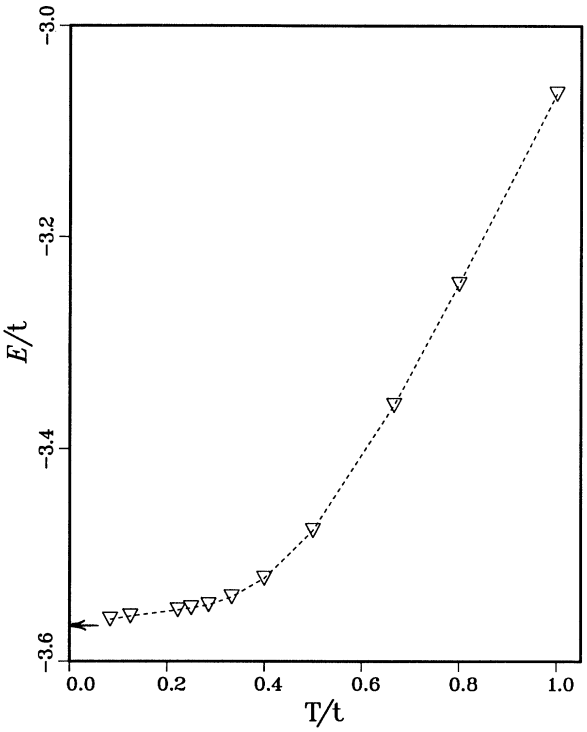

FIG. 10. Energy density E for the 4×4 cluster vs temperature T. E/t and T/t are dimensionless. ∇, simulation result. The Gutzwiller variational prediction is marked by the arrow.

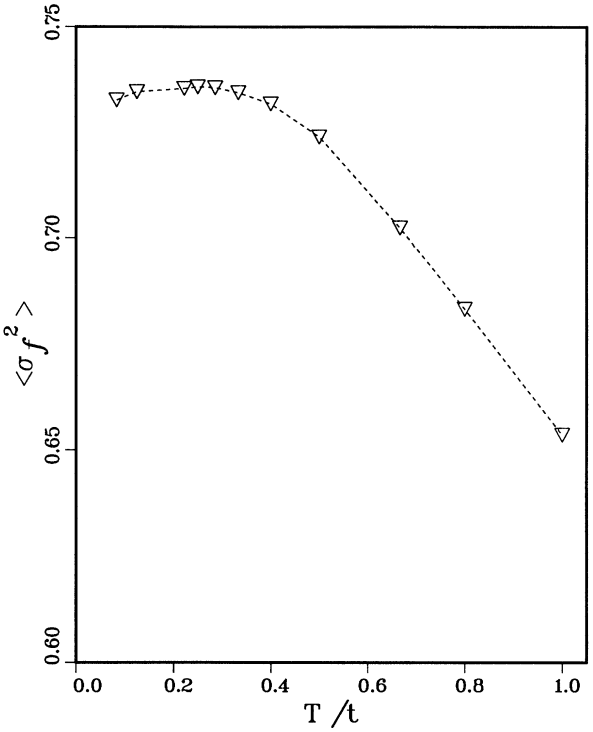

FIG. 12. f-site local moment $\langle \sigma_f^2 \rangle$ for the 4×4 cluster vs temperature T. T/t and the local moment are dimensionless. ∇, simulation result. The Gutzwiller variational prediction is marked by the arrow.

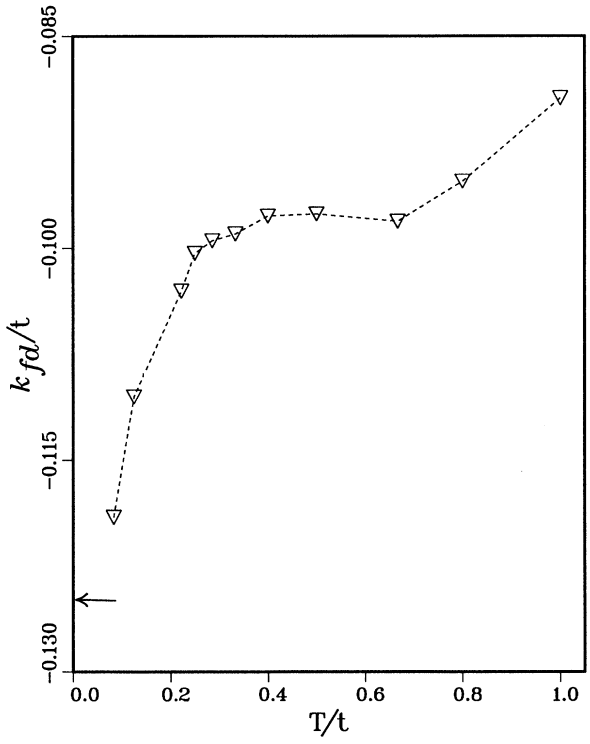

FIG. 11. Interband kinetic-energy density k_{fd} for the 4×4 cluster vs temperature T. k_{fd}/t and T/t are dimensionless. ∇, simulation result. The Gutzwiller variational prediction is marked by the arrow.

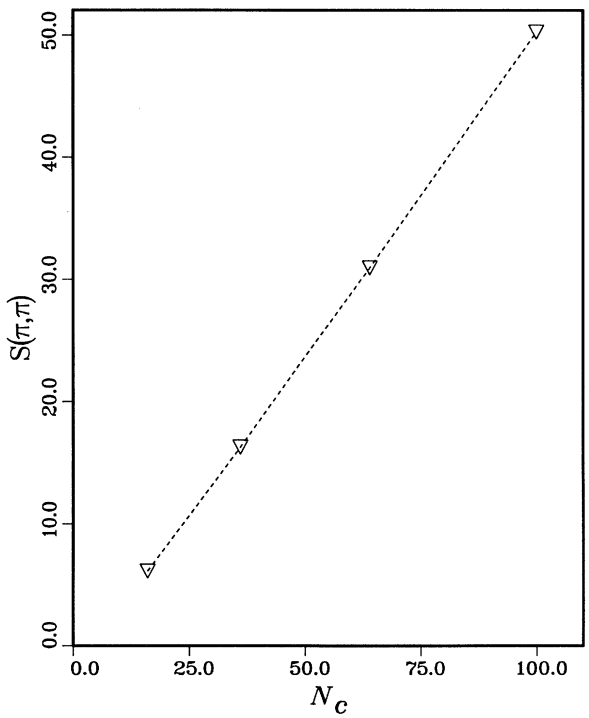

FIG. 13. $S(\pi,\pi)$ vs cluster size N_c for $U=4t$, $V=3t/8$, $E_f=-2t$, and particle density $n=2$. The cluster sizes are $4\times4=16$ unit cells, $6\times6=36$ unit cells, $8\times8=64$ unit cells, and $10\times10=100$ unit cells. $S(\pi,\pi)$ is dimensionless.

TABLE III. Comparison of simulation results and Gutzwiller variational predictions for some 4×4 clusters.

	$V=3t/8$, $E_f=-t/2$, $U=4t$	
	Simulation, $T=t/8$	Gutzwiller state
n	2.626 50	2.623 43
E_f/t	−1.549	−1.5193
n_f	1.0112	1.008 18
$\langle\sigma_f^2\rangle$	0.735	0.743
k_{fd}/t	−0.103	−0.032 73
	$V=t$, $E_f=-2t$, $U=4t$	
	Simulation, $T=2t/9$	Gutzwiller state
n	2.624 10	2.625 00
E/t	−3.548	−3.5238
n_f	1.192	1.255 01
$\langle\sigma_f^2\rangle$	0.583	0.5180
k_{fd}/t	−0.839	−0.9446

magnetic form factor $S(\mathbf{q})$ is strongly peaked at $\mathbf{q}=(\pi,\pi)$. Since $S(\mathbf{q})$ cannot be measured from the simulation, we cannot determine the magnetic correlations of the true ground state. However, our calculations suggest that the system will have strong long-range ordering; Gutzwiller states for this special choice of Hamiltonian parameters and density were determined variationally for larger cluster sizes, and $S(\pi,\pi)$ vs N_c is shown in Fig. 13 for these states. Note that $S(\pi,\pi)$ scales linearly with system size.

Away from $n=2$, the Gutzwiller ansatz does not do as well in estimating the energy for these tiny systems. This is evident in Table III, where the values of E and k_{fd} predicted by the Gutzwiller ansatz are compared with those of the simulation at $T\ll t$ for two lattices with $n\approx 2.6$ particles per unit cell. Again, the lattices are 4×4 with $U=4t$; one is a "small"-V system ($V=3t/8$ and $E_f=-t/2$), and the other is a "medium"-V system ($V=t$ and $E_f=-2t$). The energy density E determined by simulation is lower than the variational energy density for $T>0$. In particular, the two approaches differ greatly on the value of the interband kinetic energy; the Gutzwiller ansatz overestimates $|k_{fd}|$ for the medium-V system and underestimates it for the small-V system. The size of the systems examined by simulation is rather small, but recent self-consistent Green's-function calculations suggests that the Gutzwiller ansatz does indeed underestimate $|k_{fd}|$ in the small-V regime.[30]

VII. SUMMARY

Varma, Weber, and Randall[31] have characterized heavy Fermi metals with $n_f\approx 1$ as "fluctuating moment" metals, since the local moments of the f sites have not disappeared, even though they do not order. They claim that when $V^2\ll t|E_f|$, with $U\gg t$, the Gutzwiller ground state will be a heavy Fermi liquid for some particle densities $n\neq 2$. In addition, they also believe that there is an effective Ruderman-Kittel-Kasuya-Yosida (RKKY) interaction in the Gutzwiller state. Rice and Ueda, however, claimed that for such a heavy Fermi liquid to be stable against magnetic ordering, the orbital or spin degeneracy of the f bands must be large, regardless of the particle density.[32] Both research groups arrived at these rather conflicting conclusions by applying what are essentially mean-field treatments to the pseudo-partition-function of Eq. (5), a procedure that is called the Gutzwiller approximation to the Gutzwiller ansatz.

The results of our exact work, done for a spin degeneracy of two on finite-sized clusters for a variety of Hamiltonian parameters and lattice sizes, suggests that heavy Fermi liquids can be energetically stable against magnetic ordering without requiring a large spin degeneracy. Such states occur when the effective interband hopping is small and f-site occupation near 1, but the f-site local moment $\langle\sigma_f^2\rangle\approx\frac{3}{4}$. Then nearest-neighbor antiferromagnetic correlations are suppressed, and the state is very similar to the description of Varma, Weber, and Randall.[31] The spin-spin correlation peak for next-nearest neighbors, but the cluster sizes are not large enough to determine whether or not the decay length of the spin-spin correlation function has the standard RKKY form. Finite-temperature simulation of very small clusters suggests that while the Gutzwiller ansatz is a good description for the Anderson-lattice model near $n=2$, away from $n=2$ in the heavy-fermion regime, the ansatz may not properly account for the interband hopping.

ACKNOWLEDGMENTS

We wish to acknowledge helpful discussion with Sungkit Yip, Daryl Hess, and Joseph Serene. This work was supported by Grant No. DMR-89-01453 from the National Science Foundation, with additional support from the Center for Superconductivity Research at the University of Maryland. Computations were done under the auspices of the National Science Foundation at the Pittsburgh Supercomputer Center and at the Minnesota Supercomputer Center. P.G.M. also acknowledges support from the National Research Council.

[1]P. W. Anderson, Phys. Rev. **124**, 41 (1961).
[2]C. M. Varma, Phys. Rev. Lett. **55**, 2723 (1985).
[3]P. A. Lee, T. M. Rice, J. W. Serene, L. J. Sham, and J. W. Wilkens, Comments Condens. Matter Phys. **12**, 99 (1986); Peter Fulde, Joachim Keller, and Gertrud Zwicknagl, in *Theory of Heavy Fermion Systems*, Vol. 41 of *Solid State Physics*, edited by Henry Ehrenreich and David Turnbull (Academic, San Diego, 1988), p. 1.
[4]Piers Coleman, Phys. Rev. B **29**, 3035 (1984).
[5]N. Read and D. M. Newns, Solid State Commun. **52**, 993 (1984).
[6]Assa Auerbach and K. Levin, Phys. Rev. Lett. **57**, 877 (1986).

[7]A. J. Millis and P. A. Lee, Phys. Rev. B **35**, 3394 (1987).
[8]D. J. Scalapino, in *Extended Abstracts, High Temperature Superconductors, Proceedings of Symposium S, 1987 Spring Meeting of the Material Research Society,* edited by D. U. Gubser and M. Schluter (Material Research Society, Pittsburgh, 1987).
[9]Tetsuro Saso and Yutaka Seino, J. Phys. Soc. Jpn. **55**, 3729 (1986).
[10]Tetsuro Saso, Physica B&C **148**, 95 (1987).
[11]Tetsuro Saso, in *Theoretical and Experimental Aspects of Valence Fluctuations, Proceedings of the Fifth International Conference on Valence Fluctuations,* edited by L. C. Gupta and S. K. Malik (Plenum, New York, 1987).
[12]Y. Zhang and J. Callaway, Phys. Rev. B **38**, 641 (1988).
[13]Y. Zhang (private communication).
[14]M. C. Gutzwiller, Phys. Rev. Lett. **10**, 159 (1963); Phys. Rev. **134**, A923 (1964).
[15]D. Vollhardt, Rev. Mod. Phys. **56**, 99 (1984).
[16]H. Yokoyama and H. Shiba, J. Phys. Soc. Jpn. **57**, 1490 (1987).
[17]H. Shiba and H. Yokoyama, J. Phys. Soc. Jpn. **56**, 3582 (1987); Physica B **148**, 264 (1987).
[18]C. Gros, R. Joynt, and T. M. Rice, Phys. Rev. B **36**, 381 (1987).
[19]H. Shiba, J. Phys. Soc. Jpn. **55**, 2765 (1986).
[20]W. Metzner and D. Vollhardt, Phys. Rev. Lett. **59**, 121 (1987).
[21]F. Gebhard and D. Vollhardt, Phys. Rev. Lett. **59**, 1472 (1987).
[22]W. Metzner and D. Vollhardt, Phys. Rev. Lett. **62**, 324 (1989).
[23]P. G. McQueen and C. S. Wang, Phys. Rev. B **39**, 12 414 (1989).
[24]R. Blankenbecler, D. J. Scalapino, and R. L. Sugar, Phys. Rev. D **24**, 2278 (1981).
[25]J. E. Hirsch, Phys. Rev. Lett. **54**, 1317 (1985); Phys. Rev. B **31**, 4403 (1985).
[26]J. E. Hirsch, Phys. Rev. B **38**, 12 023 (1988).
[27]S. R. White, R. L. Sugar, and R. T. Scalettar, Phys. Rev. B **38**, 11 665 (1988).
[28]J. M. Luttinger, Phys. Rev. **119**, 1153 (1960).
[29]Sungkit Yip, Phys. Rev. B **38**, 8785 (1988).
[30]P. G. McQueen, J. S. Serene, and D. W. Hess (unpublished).
[31]C. M. Varma, W. Weber, and L. J. Randall, Phys. Rev. B **33**, 1015 (1986).
[32]T. M. Rice and K. Ueda, Phys. Rev. Lett. **55**, 995 (1985); Phys. Rev. B **34**, 6420 (1986).